PHYSICAL REVIEW B VOLUME 59, NUMBER 23 15 JUNE 1999-I

Doping dependence of the electronic structure of $Ba_{1-x}K_xBiO_3$ studied by x-ray-absorption spectroscopy

K. Kobayashi, T. Mizokawa, A. Ino, J. Matsuno, and A. Fujimori
Department of Physics, University of Tokyo, Hongo 7-3-1, Bunkyo-ku, Tokyo 113-0033, Japan

H. Samata, A. Mishiro, and Y. Nagata
College of Science and Engineering, Aoyama-Gakuin University, Chitosedai 6-16-1, Setagaya-ku, Tokyo 157-8572, Japan

F. M. F. de Groot
Heterogeneous Catalysis, Department of Inorganic Chemistry, University of Utrecht, 3584 CA Utrecht, The Netherlands

(Received 1 February 1999)

We have performed x-ray-absorption spectroscopy (XAS) and x-ray-photoemission spectroscopy (XPS) studies of single crystal $Ba_{1-x}K_xBiO_3$ (BKBO) covering the whole composition range $0 \leqslant x \leqslant 0.60$. Several features in the oxygen 1*s* core XAS spectra show systematic changes with *x*. Spectral weight around the absorption threshold increases with hole doping and shows a finite jump between $x=0.30$ and 0.40, which signals the metal-insulator transition. We have compared the obtained results with band-structure calculations. Comparison with the XAS results of $BaPb_{1-x}Bi_xO_3$ has revealed quite different doping dependences between BKBO and BPBO. We have also observed systematic core-level shifts in the XPS spectra as well as in the XAS threshold as functions of *x*, which can be attributed to a chemical potential shift accompanying the hole doping. The observed chemical potential shift is found to be slower than that predicted by the rigid band model based on the band-structure calculations. [S0163-1829(99)01023-1]

I. INTRODUCTION

The hole-doped bismuthate $Ba_{1-x}K_xBiO_3$ (BKBO) has been fascinating researchers since its discovery[1,2] for its diverse physical properties such as superconductivity, metal-insulator transition, and charge-density wave (CDW) formation. The crystal structure is a distorted ($0 \leqslant x < x_c$) or cubic ($x_c < x$) three-dimensional perovskite,[3] where $x_c \sim 0.38$. The parent compound $BaBiO_3$ is an insulator in contrast to the prediction of band theory that it is a metal with the half-filled nondegenerate Bi6*s*-O2*p* antibonding band crossing the Fermi level (E_F).[4–7] This discrepancy between band theory and experiment is accounted for as due to a charge disproportionation of Bi into Bi^{3+} and Bi^{5+} sites or a CDW formation accompanied by breathing and tilting distortions of the BiO_6 octahedra.[4,8,9] By increasing *x* from 0, i.e., by hole doping into $BaBiO_3$, BKBO undergoes a semiconductor-to-superconductor transition at $x=x_c$. The transition temperature (T_C) becomes highest ~ 30 K at $x=x_c$,[2] which is the highest among the copper-free oxides. It remains superconducting up to $x \sim 0.6$, above which there is a solubility limit of K atoms.[10] Those striking properties have often been compared with those of the typical cuprate system $La_{2-x}Sr_xCuO_4$ (LSCO), which also shows a transition from the insulating La_2CuO_4 into the superconducting phase with hole doping. Unlike BKBO, however, the crystal structure of LSCO is of the layered perovskite type and the parent material La_2CuO_4 is an antiferromagnetic insulator rather than a CDW insulator. It is noted that BKBO bears a close relationship with the $BaPb_{1-x}Bi_xO_3$ (BPBO) system, which shows superconductivity between $x=0$ and ~ 0.35 with the maximum T_C of ~ 12 K around $x \sim 0.25$.[11] The origin of the superconductivity in BKBO as well as in BPBO has not been settled yet: Both systems are *sp* electron systems without magnetic ions, excluding the possibility of magnetic pairing mechanisms.

Understanding the electronic structure of BKBO is a necessary step to elucidate the mechanism of its superconductivity. So far many studies have been performed on BKBO including transport, optical and tunneling experiments. Quite a few photoemission studies have also been reported[12–16] while there have been relatively few x-ray-absorption spectroscopy (XAS) studies.[17–19] XAS gives us information about the unoccupied electronic states and, therefore, is suitable for studying the effect of hole doping on the electronic structure, as has been successfully applied to LSCO.[20] Salem-sugui *et al.*[17] observed a prepeak in the O 1*s* XAS spectra for BKBO with $x=0.0$, 0.2, and 0.4 and a continuous change across the transition $x \sim x_c$ was observed. Qvarford *et al.*[18] also reported result for $x=0.1$ and 0.4 and obtained similar results. A systematic study covering a wider concentration range, however, has been lacking.

In this paper, we report on a detailed XAS study of $Ba_{1-x}K_xBiO_3$ using single crystals covering the entire available K concentration range ($0 \leqslant x \leqslant 0.60$) for the first time. Gradual and systematic *x*-dependent changes were observed for several features in the XAS spectra. We compare these results with the band-structure calculations and with the XAS results of BPBO. A quantitative analysis has been made on the spectral weight of the prepeak. Contrasting doping behaviors have been revealed between BKBO and BPBO. We also performed XPS measurements on the core levels of BKBO. The observed core-level shifts will be discussed in terms of the chemical potential shift due to the hole doping.

II. EXPERIMENTS

$Ba_{1-x}K_xBiO_3$ single crystals ($x=0.10$, 0.20, 0.30, 0.40, 0.50, and 0.60) were grown by an electrochemical method from a KOH solution with $Ba(OH)_2\cdot 8H_2O$ and Bi_2O_3. The composition of each sample was determined by EPMA.[21] A $BaBiO_3$ single crystal was prepared by the flux method.

XAS measurements were performed at beamline BL-2B of Photon Factory, High Energy Accelerator Research Organization. Photon energies were calibrated using the Cu $2p_{3/2}$ edge of Cu metal at 932.5 eV (Ref. 22) and the O $1s$ edge of $LaCoO_3$ at 529.3 eV.[23] O $1s$ XAS spectra were taken by the total electron-yield method with photoelectrons. The energy resolution including the lifetime of the O $1s$ core hole was ~ 0.7 eV at 530 eV. The samples were cooled down to ~ 50 K using a closed-cycle He refrigerator. The pressure in the spectrometer was $\sim 4\times 10^{-10}$ Torr.

XPS measurements were performed using the Mg Kα line ($h\nu=1253.6$ eV) and photoelectrons were collected using a PHI DCMA. Calibration and estimation of the instrumental resolution were done using gold evaporated on the sample surface defining Au $4f_{7/2}=84.0$ eV. The total resolution was ~ 1 eV, including both the light source and the instrumental resolution. The base pressure in the spectrometer was $\sim 6\times 10^{-10}$ Torr. All the XPS measurements were performed at room temperature in order to avoid charging effect in the insulating phase.

The samples were scraped *in situ* with a diamond file for both measurements. For the XAS measurements, which are less surface sensitive than XPS, samples were scraped until the spectra showed no further change. The obtained XAS spectra seem consistent with the previous reports for $x=0$ (Ref. 24) and $x=0.40$.[19] For the XPS measurements, scraping was performed until the O $1s$ core-level spectra became a single peak. We confirmed that the measured peak intensity of the Ba $3d$ XPS core level was proportional to x, while those of the O $1s$ and Bi $4f$ core levels were almost independent of x.

III. RESULTS AND DISCUSSION

A. Overall electronic structure of the unoccupied states

Figure 1 shows the XAS spectra of $Ba_{1-x}K_xBiO_3$ for various x's. We superimpose the spectrum of $BaBiO_3$ ($x=0.00$) on each spectrum ($x\geqslant 0.10$) as a solid curve. Normalization of all the spectra was performed by peak height at the photon energy $h\nu=533$–535 eV. In the bottom, difference spectra from the $BaBiO_3$ spectrum are shown. Notable structures found in the spectra are labeled as a–f in Fig. 1, and the positions of structures a–e are plotted in Fig. 2.

The O $1s$ XAS spectra represent the unoccupied partial density of states (PDOS) of p character at the oxygen site. Structure a near the absorption edge $h\nu\sim 528.0$–528.5 eV grows almost monotonously as x increases, which is also substantiated in the bottom panel of Fig. 1. At $x=0.00$, the shape of the prepeak a is rounded, while it becomes a sharper peak at $x\geqslant 0.10$. For the spectra $0.10\leqslant x\leqslant 0.30$, where BKBO is insulating, the peak grows slowly as x increases. At $x=0.40>x_c$, where BKBO enters the metallic region, the prepeak suddenly becomes intense and keeps its height until $x=0.60$. The increase of the prepeak is due to the doped holes and the rapid growth from $x=0.30$ to 0.40 would be attributed to a transfer of spectral weight to the region near the chemical potential, signaling the metal-insulator transition. This behavior is essentially different from that in LSCO,[20] where new spectral weight appears well below the first peak of the insulator La_2CuO_4. A quantitative discussion about the spectral weight of the prepeak will be made in Sec. III C.

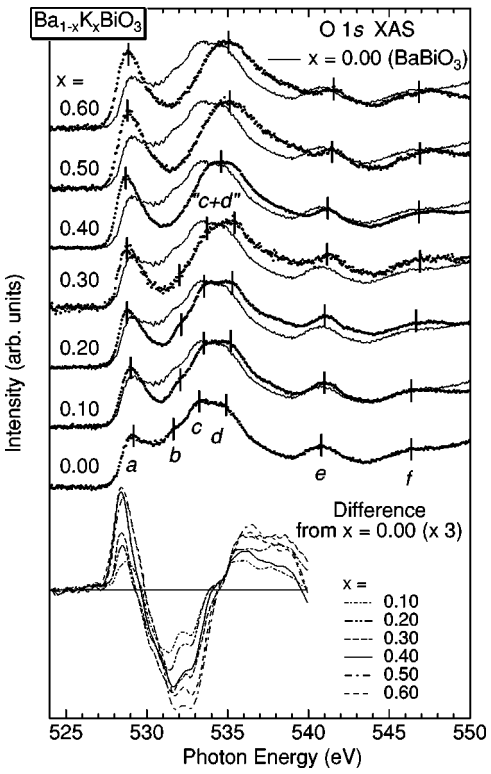

FIG. 1. Oxygen $1s$ x-ray-absorption spectra (XAS) of a series of $Ba_{1-x}K_xBiO_3$ ($0\leqslant x\leqslant 0.60$). The spectrum of $BaBiO_3$ is superimposed on each spectrum as a solid curve. They are normalized to their peak height around $h\nu=533$–535 eV. The positions of a–e are plotted in Fig. 2. In the bottom panel are shown the difference spectra from the XAS spectrum of $BaBiO_3$.

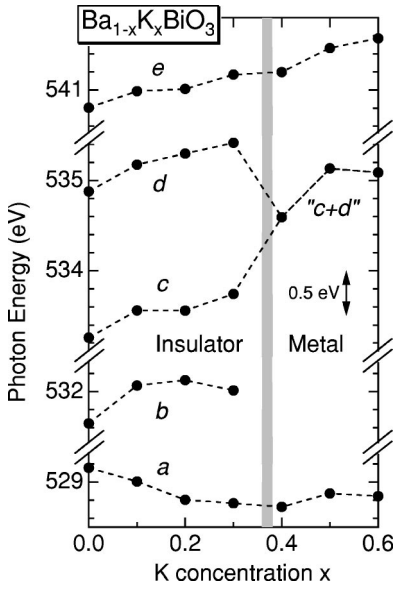

FIG. 2. Positions of structures a–e indicated in Fig. 1.

Next, we investigate the behaviors of structures b–f. Structure b, which appears as a shoulderlike structure for $x=0.00$ at $h\nu\sim532$ eV, becomes obscure in going from $x=0.00$ to 0.30 and disappears at $x\geqslant0.40$. Hence, b may be attributed to Ba character, which point will be discussed below. The behavior of structure c at $h\nu\sim533$–534 eV and structure d at $h\nu\sim535$ eV is also systematically dependent on x. At $x=0.00$, feature c with a slightly smaller feature d is observed. This two-component peak centered around $h\nu\sim534$ eV is monotonously shifted to higher photon energies with x, until the center of the peak reaches $h\nu\sim535$ eV. At the same time, d becomes stronger than c at $x\sim0.30$ and, finally, structures c and d merge at $x\geqslant0.40$ into a peak as labeled ''$c+d$'' in Figs. 1 and 2. This observation can be explained as follows: Structures c and d are mainly of Ba character at $x=0.00$, while the substituted states of K character appear at the position of d for $x\geqslant0.10$ and, therefore, the gradual change results from the change of the electronic structure due to the substitution of K for Ba. As will be discussed in Sec. III B, this is also supported by the result of the XAS spectra of BPBO,[24] where the corresponding c structure does not move to higher photon energies so much as that in BKBO.

Besides a–d, the behaviors of the structures in the higher photon energy region are worth mentioning although they behave less drastically than those near the absorption edge. On one hand, structure e around $h\nu\sim541$ eV simply becomes weak with x, indicating that this structure is of Ba character. On the other hand, the broader structure f around $h\nu\sim547$ eV does not change in the entire x range, indicating this to be of Bi or purely of O character.

It is interesting to compare these observations with the previous report on the unoccupied states of BKBO studied by inverse photoemission spectroscopy. Wagener *et al.*[16] assigned structures at about 4, 7, 9, and 14 eV above E_F (corresponding structures b–e) to Bi $6p$, Ba $5d$, K $3d$, and Ba $4f$ states, respectively. As for structures c, d, and e, their assignment agrees with ours. If b is assigned to the Bi $6p$ band as they identified, our observation that b disappears at $x\geqslant0.40$ may indicate a change of the electronic structure caused by the change of the crystal structure.

In Fig. 3, we show comparison between the XAS spectra of $BaBiO_3$ and $Ba_{0.9}K_{0.1}BiO_3$ and the theoretical spectrum of $BaBiO_3$ derived from the unoccupied oxygen p PDOS.[5] The oxygen PDOS has been broadened with a Gaussian and a Lorentzian which represent the instrumental resolution ~0.5 eV and the lifetime broadening of O $1s$ core hole ~0.3 eV, respectively.[24] The energy scale of the theoretical spectrum has been shifted so as to compare well with the experimental spectra. Structures in the theoretical spectrum are labeled as α–γ. Although the line shapes of the XAS spectra tend to be distorted by the core-hole potential, the theoretical spectrum reproduces experiment to some extent: Structures α, β, and γ seem to correspond to a, b, and c (or d), respectively. In addition, it is interesting to note that, as for the prepeak a, the theoretical spectrum resembles the experimental spectrum of $Ba_{0.9}K_{0.1}BiO_3$ rather than that of $BaBiO_3$. Because both samples are insulating, this cannot be explained only by the effect of the core-hole potential. This may be related to the difference of the crystal structure between $x=0.00$ and $x=0.10$ since the strong breathing-type distortion and the tilting of the BiO_6 octahedra exist for $x\leqslant0.1$ with a large electron-phonon coupling constant.[3,9]

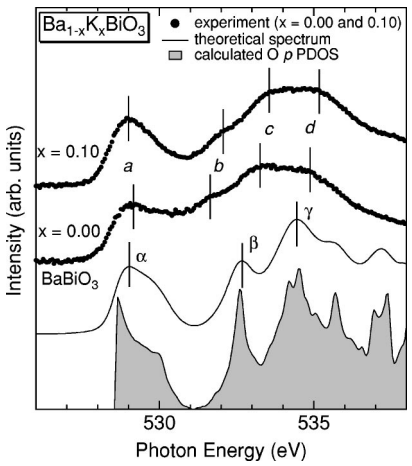

FIG. 3. Comparison of the XAS spectra of $BaBiO_3$ and $Ba_{0.9}K_{0.1}BiO_3$ (dots) with the theoretical spectrum (solid curves) derived from the unoccupied O p PDOS (Ref. 5). The labels a–d are the same as in Fig. 1.

B. Comparison with the XAS spectra of $BaPb_{1-x}Bi_xO_3$

Next we compare our results with the previous report on the XAS spectra of the BPBO system.[24] In the upper panel of Fig. 4, the XAS spectra of a series of $BaPb_{1-x}Bi_xO_3$ ($0.0\leqslant x\leqslant1.0$) are shown by dots, with the $BaBiO_3$ XAS spectrum superimposed for comparison.[25] All the spectra have been normalized to their peak height around $h\nu\sim534$ eV.

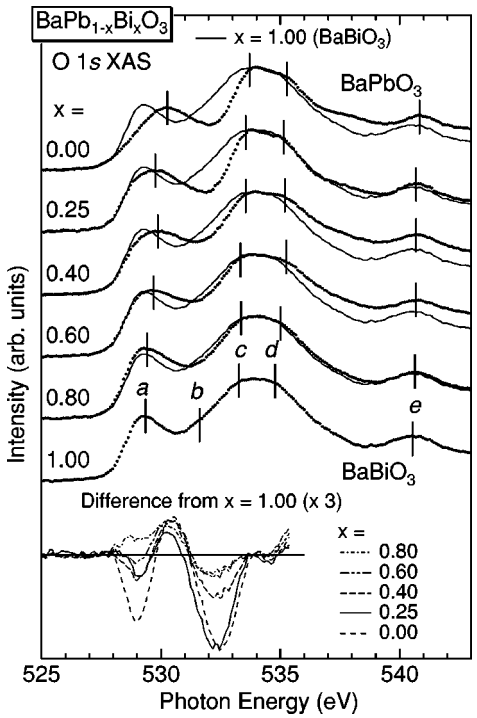

FIG. 4. O $1s$ XAS spectra of a series of $BaPb_{1-x}Bi_xO_3$ ($0.0\leqslant x\leqslant1.0$). The spectrum of $BaBiO_3$ is superimposed on each spectrum. They are normalized to their peak height around $h\nu=534$ eV. The positions of a–e are plotted in Fig. 5. In the bottom panel are shown the difference spectra from that of $BaBiO_3$.

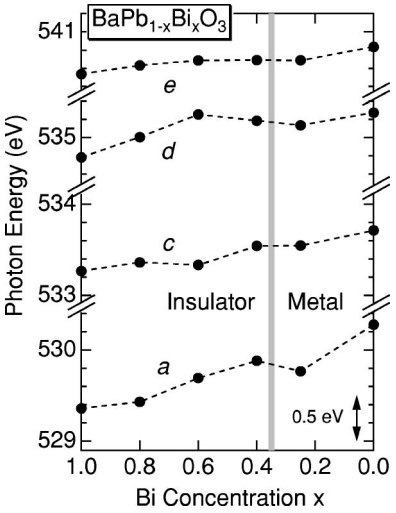

FIG. 5. Positions of structures a and c–e indicated in Fig. 4.

We have labeled structures as a–e. In the bottom, the difference spectra from the $BaBiO_3$ spectrum are shown. The positions of structures a–e are plotted in Fig. 5.

Although structure b is only weekly visible, structures c, d, and e correspond well to those of BKBO in Fig. 1. Unlike BKBO, c and d do not greatly change their positions and line shapes with x. e also does not change its position with x. This supports the above assignment for BKBO that c, d, and e are mainly of Ba character. On the other hand, the position and line shape of the prepeak labeled a changes dramatically with x, while their intensity relative to the main peak at $h\nu = 533$–535 eV is conserved. This observation is clearly contrasted with the case of BKBO, where the intensity of the prepeak increases with x. The difference spectra in the bottom panel also clarify this point. As for BPBO, the intensity of the prepeak a a little increases in going from $x=1.00$ to 0.80, and then decreases almost monotonously as x decreases. Unlike BKBO, there is another structure in the difference spectra at $h\nu \sim 530$ eV, which does not behave systematically, while the broad dip at ~ 532–533 eV increases with decreasing x. Such complicated behaviors significantly differ from those of BKBO, reflecting the different doping processes between BPBO and BKBO. In the former system, the Bi $6s$–O $2p$ antibonding band is replaced by the Pb $6s$–O $2p$ antibonding band near E_F. In the latter system, the doped holes are rather simply accommodated in the Bi $6s$–O $2p$ antibonding band. The different doping processes are also reflected on the opposite shifts of peak a in BKBO and BPBO (Figs. 2 and 5). Other structures are shifted more slowly in BPBO than in BKBO.

C. Electronic structure near the Fermi level

In this section, we discuss how doped holes are accommodated in the Bi $6s$–O $2p$ antibonding band in BKBO based on the doping dependence of the intensity of the prepeak. In order to characterize how the prepeak grows with K substitution, the peak around $h\nu = 534$–535 eV has been subtracted by assuming it to be a Gaussian, as shown in Fig. 6(a). Here, the shaded area represents the extracted prepeak. In Fig. 6(b), the area $N(x)$ of the prepeak relative to that of the Gaussian is plotted as a function of x. We have scaled

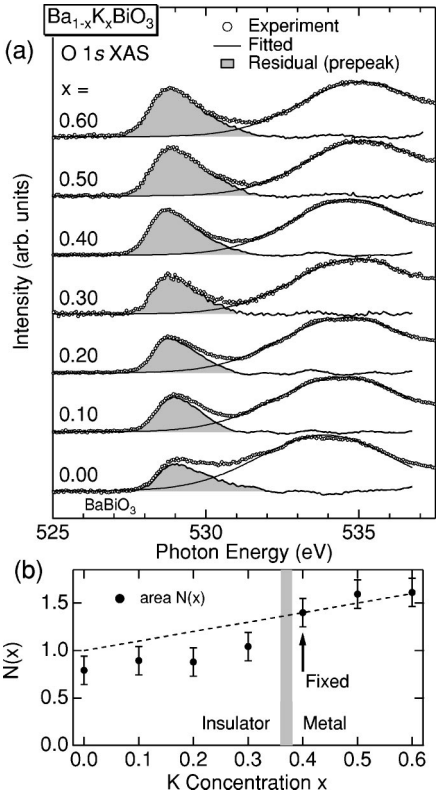

FIG. 6. (a) Prepeak of the XAS spectra extracted on the assumption that the peak at $h\nu = 534$–535 eV is a Gaussian. (b) Area $N(x)$ of the prepeak relative to that of the main peak. $N(x)$ has been normalized assuming that $N(x=0.40)=1.40$. The dashed line represents the ''ideal hole doping'' as explained in the text.

$N(x)$ so that $N(x=0.40)=1.40$ because $N(x)$ would be proportional to the number of empty states in the Bi $6s$–O $2p$ antibonding band if the strength of the Bi $6s$–O $2p$ hybridization does not change with x.

In accordance with the observation in Fig. 1 that the prepeak grows systematically with x, the extracted $N(x)$ is a monotonously increasing function of x in the whole x range. The dashed line in Fig. 6(b) represents the ''ideal hole doping'' $N(x)=1+x$. One can see a deviation from this ''ideal'' behavior below $x=0.30$ with a jump between $x=0.30$ and 0.40, i.e., below and above $x=x_c$. The present result suggests that below $x=x_c$, doped holes may not be accommodated in the Bi $6s$–O $2p$ antibonding band in the same way as in the metallic phase, resulting in the reduced $N(x)$ and the insulating behavior. In other words, spectral weight due to the empty Bi $6s$–O $2p$ states, which should be proportional to $1+x$, is not concentrated near E_F, but is also distributed away from E_F, presumably overlaid by the Gaussian.

Next, we focus on the shift of the threshold of the XAS spectra. Figure 7(a) shows the XAS spectra of BKBO near the absorption threshold. We define the threshold by the midpoint of the leading edge as marked by the vertical bars in the figure. The result of the threshold shift is shown in the bottom panel of Fig. 8. The positions of the prepeak a around $h\nu \sim 529$ eV are also indicated by vertical bars in Fig. 7(a). In going from $x=0.00$ to 0.20, the prepeak position rapidly moves toward lower photon energies as shown in Fig. 2. On the other hand, the threshold is shifted more slowly than that

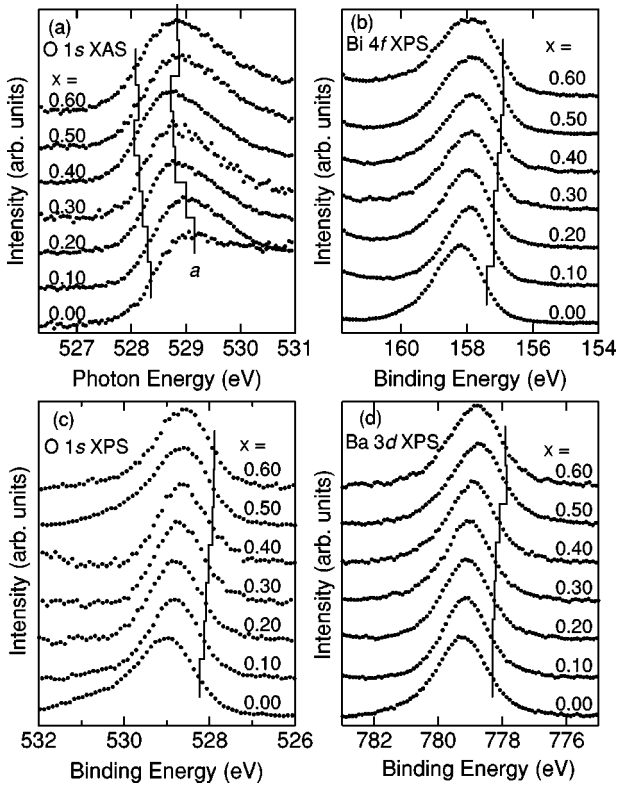

FIG. 7. (a) O $1s$ XAS spectra of BKBO near the absorption threshold. The threshold defined as the midpoint of the peak are marked with vertical bars. The position of the prepeak a is also shown. (b), (c), and (d) are the XPS spectra of the Bi $4f$, O $1s$, and Ba $3d$ core levels. The midpoint of the peak is marked with the vertical bars. In each panel, the spectra have been normalized to the peak height.

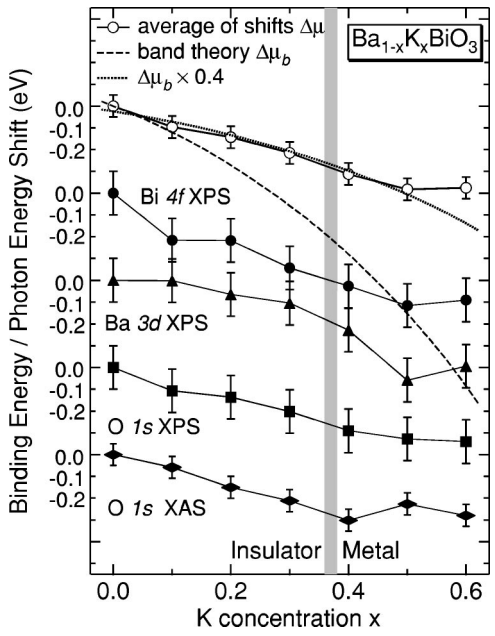

FIG. 8. Shifts of the O $1s$ XAS threshold and the O $1s$, Ba $3d$, and Bi $4f_{7/2}$ XPS core levels. In the top, the average shift of the XAS threshold and the XPS core levels and the theoretical chemical potential shift calculated by band theory (Ref. 5) assuming the rigid band model are shown.

of the prepeak in going from $x=0.00$ to $x=0.20$, meaning that the prepeak becomes broader with decreasing x. This may have an origin common with the depression of the spectral weight $N(x)$ in the insulating phase and may be attributed to the structural distortion and the CDW gap formation in the insulating phase. It has been reported in the optical study that the CDW gap of ~ 2 eV opens at $x=0.00$, while it almost collapses already at $x=0.24$.[26] On the other hand, in the metallic region at $x \geqslant 0.40$, the shift of the XAS threshold seems almost saturated. This saturation may arise from the difficulty in the definition of the threshold in the metallic region because of the pile-up of spectral weight near E_F, since the O $1s$ XPS peak shift behaves systematically for $x \leqslant 0.50$ as reported below.

The depression of $N(x)$ in the insulating phase implies a possible failure of the simple rigid-band model. In this region, doped holes would be localized due to strong electron-phonon coupling, which decreases the spectral weight near E_F. This is consistent with the report by Puchkov *et al.*[27] that spectral weight observed in the midinfrared absorption of the insulating BKBO is suppressed and that the lost spectral weight is transferred to a higher energy region. In contrast, above $x=x_c$, spectral weight of the holes introduced by the substitution of K for Ba are distributed near E_F, leading to the regular behavior of $N(x)$.

D. Core-level XPS spectra and chemical potential shift

In Figs. 7(b), 7(c), and 7(d), we also show the results of the Bi $4f_{7/2}$, O $1s$ and Ba $3d$ core-level XPS spectra, respectively. According to the high resolution XPS study,[18] the line shapes of the core levels of the metallic BKBO are not single peaks but of multicomponents with an energy-loss structure on the high binding energy (E_B) side. In fact, the core-level spectra in the metallic phase (particularly, $x=0.50$ and 0.60) show somewhat broader peak widths than those in the insulating phase. In order not to be disturbed by such energy-loss structures, we use the midpoint of the lower binding energy edge of each peak. The peak positions thus obtained are shown by vertical bars in Figs. 7(b), 7(c), and 7(d). The results of the Bi $4f_{7/2}$, O $1s$, and Ba $3d$ core-level binding energies relative to $x=0.00$ are compiled in Fig. 8. In going from $x=0.00$ to 0.50,[28] each core level gradually moves to lower E_B by ~ 0.3–0.5 eV. The direction and amount of the core-level shifts are common to all the core levels in agreement with the previous result.[14] Between $x=0.00$ and 0.40, the shift of the O $1s$ core-level XPS spectrum and the shift of the threshold of the O $1s$ XAS spectrum agree with each other quite well, indicating that the XAS threshold corresponds to a transition from the O $1s$ core level to states at E_F.

Here, it is important to note that the core levels of both anion (O) and cations (Ba, Bi) move in the same direction, indicating that the observed shift is a measure of the chemical potential shift caused by the hole doping. We have obtained the average of the shifts of the O $1s$ XAS threshold and the XPS core levels of Ba $3d$, O $1s$, and Bi $4f$ as plotted by open circles in Fig. 8 and regard it as the experimentally deduced chemical potential shift $\Delta\mu(x)$. Except for $x=0.60$, $\Delta\mu(x)$ decreases monotonously. In Fig. 8, we have also plotted the chemical potential shift $\Delta\mu_b(x)$ predicted by

the band-structure calculations based on the rigid band model[5] by a dashed curve. The qualitative behavior of $\Delta\mu(x)$ implies that the doping dependence of the BKBO system obeys the rigid band model, as pointed out before by Namatame *et al.*[14] Quantitatively, however, the amount of $\Delta\mu(x)$ is reduced compared to $\Delta\mu_b(x)$, indicating that the rigid band model based on the band-structure calculations does not succeed in the quantitative explanation of $\Delta\mu(x)$. In fact, we found that $0.4\times\Delta\mu_b(x)$ well reproduces the $\Delta\mu(x)$ as shown by a dotted line in the figure. Zakharov *et al.*[15] observed a 0.35 eV shift of the O $2p$ band between $x=0.1$ and 0.4 by photoemission spectroscopy, corresponding to the factor of ~ 0.6. Namatame *et al.*[14] also reported that the measured chemical potential shift is reduced almost to half of the theoretical prediction.

Finally, it should be noted that the behavior of $\Delta\mu(x)$ is gradual without any abruptness across $x=x_c$, which is in clear contrast to the fact that there is a finite jump in the prepeak area $N(x)$ between $x=0.30$ and 0.40. These two facts may be related to the opening of the pseudogap in the metallic samples.[14] This is an issue to be clarified in the future.

IV. CONCLUSION

We have performed XAS and XPS measurements of BKBO in the whole x range ($0\leqslant x\leqslant 0.60$). The XAS results show that the overall electronic structure of the unoccupied states changes systematically with substitution of K for Ba. That is, the intensity of the prepeak increases monotonously with a finite jump between $x=0.30$ and 0.40, and the absorption threshold moves toward lower energies, at least in the insulating phase. Good overall agreement with the band-structure calculations has been obtained. Comparison with the XAS result of the BPBO system has revealed very different doping-dependent changes in the electronic structure between BKBO and BPBO. In the latter system, Pb substitution replaces the prepeak in $BaBiO_3$ of Bi $6s-$O $2p$ antibonding character by another peak of Pb $6s$ character at a higher energy. The XPS measurements reveal that the chemical potential shift $\Delta\mu(x)$ derived from the core-level shifts moves in the direction predicted by the rigid-band model. The amount of the shift, however, is almost half of that predicted by the band-structure calculations.

ACKNOWLEDGMENTS

The authors would like to thank Y. Azuma, T. Miyashita, and the staff of Photon Factory for technical support in the XAS measurements. We would like to thank H. Takagi for providing us with the $BaBiO_3$ sample and T. Hashimoto for informative discussions. This work was supported by a Special Coordination Fund from the Science and Technology Agency of Japan. One of us (K.K.) would like to thank the Japan Society for the Promotion of Science for Young Scientists for financial support. The experiment at Photon Factory was done under the approval of the Photon Factory Program Advisory Committee (Proposal No. 94-G361).

[1] L. F. Mattheiss, E. M. Gyorgy, and D. W. Johnson, Jr., Phys. Rev. B **37**, 3745 (1988).

[2] R. J. Cava, B. Batlogg, J. J. Krajewski, R. Farrow, L. W. Rupp, Jr., A. E. White, K. Short, W. F. Peck, and T. Kometani, Nature (London) **332**, 814 (1988).

[3] Shiyou Pei, J. D. Jorgensen, B. Dabrowski, D. G. Hinks, D. R. Richards, A. W. Mitchell, J. M. Newsam, S. K. Sinha, D. Vaknin, and A. J. Jacobson, Phys. Rev. B **41**, 4126 (1990).

[4] L. F. Mattheiss and D. R. Hamann, Phys. Rev. B **28**, 4227 (1983).

[5] K. Takegahara and T. Kasuya, J. Phys. Soc. Jpn. **56**, 1478 (1987).

[6] L. F. Mattheiss and D. R. Hamann, Phys. Rev. Lett. **60**, 2681 (1988).

[7] N. Hamada, S. Massidda, A. J. Freeman, and J. Redinger, Phys. Rev. B **40**, 4442 (1989).

[8] D. E. Cox and A. W. Sleight, Solid State Commun. **19**, 969 (1976).

[9] A. I. Liechtenstein, I. I. Mazin, C. O. Rodriguez, O. Jepsen, O. K. Andersen, and M. Methfessel, Phys. Rev. B **44**, 5388 (1991).

[10] T. Uchida, Doctor Thesis, Aoyama-Gakuin University, 1995.

[11] S. Tajima, S. Uchida, A. Masaki, H. Takagi, K. Kitazawa, S. Tanaka, and A. Katsui, Phys. Rev. B **32**, 6302 (1985); S. Tajima, S. Uchida, A. Masaki, H. Tagaki, K. Kitazawa, S. Tanaka, and S. Sugai, *ibid.* **35**, 696 (1987); C. Chaillout, A. Santoro, J. P. Remeika, A. S. Cooper, G. P. Espinosa, and M. Marezio, Solid State Commun. **65**, 1363 (1988).

[12] M. W. Ruckman, D. Di Marzio, Y. Jeon, G. Liang, J. Chen, M. Croft, and M. S. Hegde, Phys. Rev. B **39**, 7359 (1989).

[13] M. Nagoshi, T. Suzuki, Y. Fukuda, K. Ueki, A. Tokiwa, M. Kikuchi, Y. Syono, and M. Tachiki, J. Phys.: Condens. Matter **4**, 5769 (1992).

[14] H. Namatame, A. Fujimori, H. Torii, T. Uchida, Y. Nagata, and J. Akimitsu, Phys. Rev. B **50**, 13 674 (1994).

[15] A. A. Zakharov, U. Johansson, M. Leandersson, H. Nylén, M. Qvarford, I. Lindau, and R. Nyholm, Phys. Rev. B **56**, R5755 (1997).

[16] T. J. Wagener, H. M. Meyer III, D. M. Hill, Y.-J. Hu, M. B. Jost, J. H. Weaver, D. G. Hinks, B. Dabrowski, and D. R. Richards, Phys. Rev. B **40**, 4532 (1989).

[17] S. Salem-Sugui, Jr., E. E. Alp, S. M. Mini, M. Ramanathan, J. C. Campuzana, G. Jennings, M. Faiz, S. Pei, B. Dabrowski, Y. Zheng, D. R. Richards, and D. G. Hinks, Phys. Rev. B **43**, 5511 (1991).

[18] M. Qvarford, V. G. Nazin, A. A. Zakharov, M. N. Mikheeva, J. N. Andersen, M. K.-J. Johansson, G. Chiaia, T. Rogelet, S. Söderholm, O. Tjernberg, H. Nylén, I. Lindau, R. Nyholm, U. O. Karlsson, S. N. Barilo, and S. V. Shiryaev, Phys. Rev. B **54**, 6700 (1996).

[19] H. Nylén; A. Beutler, A. A. Zakharov, M. Leandersson, M. Qvarford, I. Lindau, M. B. Tsetlin, L. L. Lev, M. N. Mikheeva, S. N. Barilo, and S. V. Shiryaev, Phys. Rev. B **58**, 12 836 (1998).

[20] C. T. Chen, F. Sette, Y. Ma, M. S. Hybertsen, E. B. Stechel, W. M. C. Foulkes, M. Schluter, S.-W. Cheong, A. S. Cooper, L. W. Rupp, Jr., B. Batlogg, Y. L. Soo, Z. H. Ming, A. Krol, and Y. H. Kao, Phys. Rev. Lett. **66**, 104 (1991).

[21] Y. Nagata, N. Suzuki, T. Uchida, W. D. Mosley, P. Klavins, and R. N. Shelton, Physica C **195**, 195 (1992); T. Uchida, S. Naka-

mura, N. Suzuki, Y. Nagata, W. D. Mosley, M. D. Lan, P. Klavins, and R. N. Shelton, *ibid.* **215**, 350 (1993).

[22] M. Grioni, J. B. Goedkoop, R. Schoorl, F. M. F. de Groot, J. C. Fuggle, F. Schäfers, E. E. Koch, G. Rossi, J.-M. Esteva, and R. C. Karnatak, Phys. Rev. B **39**, 1541 (1989).

[23] T. Saitoh, T. Mizokawa, A. Fujimori, M. Abbate, Y. Takeda, and M. Takano, Phys. Rev. B **56**, 1290 (1997).

[24] F. M. F. de Groot, J. C. Fuggle, and J. M. van Ruitenbeek, Phys. Rev. B **44**, 5280 (1991).

[25] Here, we have linearly rescaled the photon energies of the spectra measured by de Groot *et al.* (Ref. 24) so that their $BaBiO_3$ result agrees well with ours except for the slightly better energy resolution in the present data. This discrepancy may be due to a technical reason, namely, the method of the photon energy calibration.

[26] M. A. Karlow, S. L. Cooper, A. L. Kotz, M. V. Klein, P. D. Han, and D. A. Payne, Phys. Rev. B **48**, 6499 (1993).

[27] A. V. Puchkov, T. Timusk, M. A. Karlow, S. L. Cooper, P. D. Han, and D. A. Payne, Phys. Rev. B **54**, 6686 (1996).

[28] The singular behavior at $x = 0.60$ might be due to the fact that the sample is near the solubility limit of K in the BKBO system.